Master’s Thesis of Mechanical Engineering

Performance Evaluation and Adjustment of Spherical Mechanism in Hip Exoskeleton Robot for Centroid Alignment

고관절 외골격 로봇의 중심 정렬을 위한 구면 메커니즘의 성능 평가 및 조정

August 2023

Graduate School of Mechanical Engineering
Seoul National University

Gyuik Lee

Performance Evaluation and Adjustment of Spherical Mechanism in Hip Exoskeleton Robot for Centroid Alignment

Advisor Yoon Young Kim

Submitting a master's thesis of
Mechanical Engineering

April 2023

Graduate School of Mechanical Engineering
Seoul National University

Gyuik Lee

Confirming the master's thesis written by
Gyuik Lee

June 2023

Chair	Do-Nyun Kim	(Seal)
Vice Chair	Yoon Young Kim	(Seal)
Examiner	Jinkyu Yang	(Seal)

ABSTRACT

Performance Evaluation and Adjustment of Spherical Mechanism in Hip Joint Exoskeleton Robot for Centroid Alignment

Gyuik Lee

School of Mechanical and Aerospace Engineering

The Graduate School

Seoul National University

Misalignment between the center of rotation of a human joint and a robot joint can have a significant impact in terms of efficiency and safety. However, due to the hip joint's high degree of freedom and the fact that its rotation center is located inside the body, the probability of this occurring is relatively high. This study proposes a new methodology to predict the exact location of the hip joint using only the internal sensors. A testbench that can intentionally impose misalignment was constructed, and an R-4bar-R (R4R) spherical mechanism was used to validate this method. By using the correlation of output moment and misalignment, a mapping system was created so that the misalignment could be back-estimated. Gaussian Process Regression was employed to construct the model.

Keywords: Exoskeleton Robot, Hip Joint, Misalignment Prediction, Calibration Methodology, Testbench, Strain Gauge Wheatstone Bridge, Spherical Mechanism, Latin Hypercube Sampling, Gaussian Process Regression

Student Number: 2021-20088

CONTENTS

LIST OF TABLES

LIST OF FIGURES

CHAPTER 1.
INTRODUCTION

1.1 Motivation

Interest in exoskeleton technology is increasing with strong momentum worldwide in the robotics industry. An exoskeleton device is a robotic system that enhances the wearer's mobility by exerting physical force beyond their inherent capabilities. It has been rapidly developed and commercialized in various fields such as military and disability assistance [1][2], and has also been applied to most significant joints of the human body [3][4]. For these robots to fulfill their intended function, proper alignment with the human body is necessary. However, the occurrence of misalignment between the axis of rotation in the robotic joint and human joint can result in reduced efficiency, lack of output power, or even safety issues.

Joints with three degrees of freedom (DOF), such as the hip joint or shoulder, have difficulty finding the exact location compared to other 1 DOF joints, like knees and elbows. This is attributed to the fact that the joint's center of rotation is located inside the body as a singular point and also due to the variability in individuals' body shape and sizes. Since these difficulties can lead to misalignment, research to find the exact location of the center of rotation of the hip joint has been ongoing.

1.2 Previous Works

The common ways many previous studies used to find the hip joint are to X-ray the whole body [5], or to computationally predict the joint using the bones that are easily recognizable from the outside [6]. For the first method, while it may make accurate identification in static cases such as a standing posture before walking, the accuracy may not be feasible in dynamic situations such as during a walking process because the instantaneous center of rotation does not remain at the same point. The second method, which uses markers on the body and motion capture cameras, can position even in dynamic environments, but can only be used in environments where experimental equipment such as cameras are built. Thus, it was determined that there is currently a lack of research on methods for precisely determining the position of the hip joint in dynamic environments, free from environmental influences.

1.3 Research Objectives

Real-time detection of varying misalignment during walking is crucial for an exoskeleton robot, yet there is a limited number of methods available for achieving this. While some approaches rely on external markers, their applicability is restricted to confined spaces. In contrast, the proposed method offers a solution by leveraging real-time data extraction to estimate misalignment, thereby overcoming the aforementioned limitations.

This paper introduces a novel methodology for determining the position of the hip joint by using the ratio of three components of output moment. A testbench capable of intentionally applying misalignments was constructed, and the resulting moments under various misalignment conditions were analyzed. We used an R-4bar-R mechanism (Fig. 1.1 (a)) [7] which produces 3 dimensional moments from a single axis input moment (Fig. 1.1 (b)). Based on the experimental data from the testbench, a mapping system was constructed, so that when output moment is inserted, a corresponding prediction of misalignment can be produced. The experimental predicted value is subsequently cross-validated against the actual misalignment value, thus establishing the credibility and reliability of this study.

(a) (b)

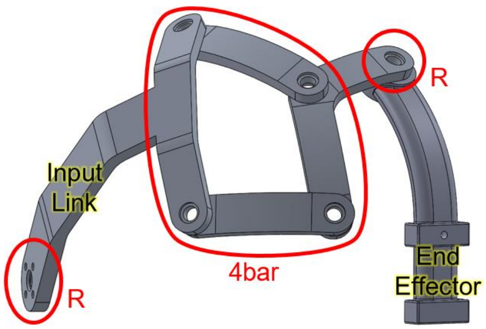

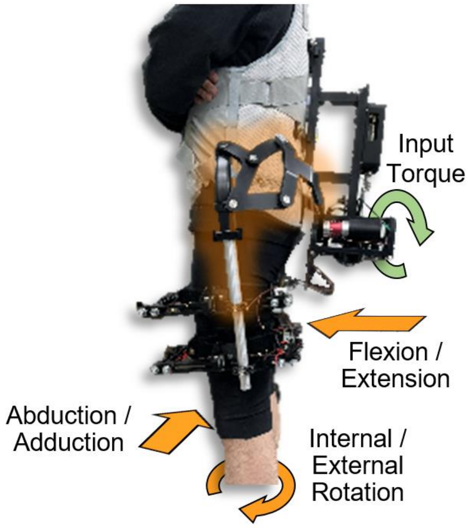

Fig. 1.1 A R-4bar-R spherical mechanism was used in this study [7]. (a) 3D model of mechanism. (b) A complete image of the robot with the mechanism attached.

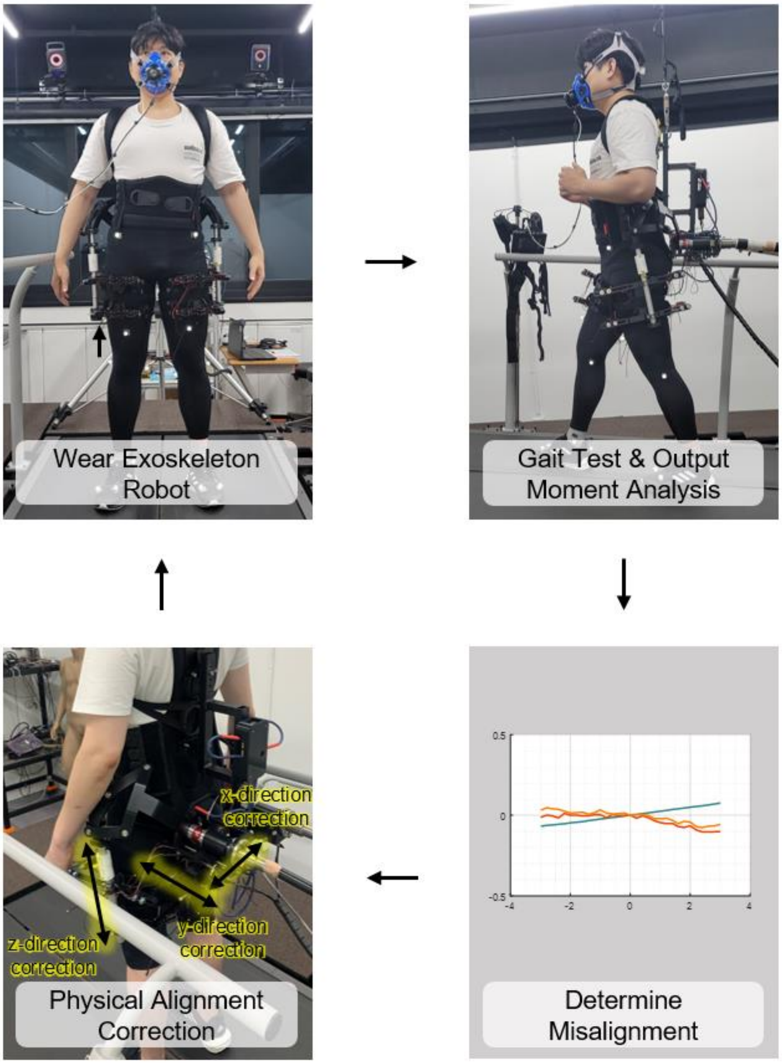

Fig. 1.2 An overall schematic diagram illustrating the implementation of the proposed novel methodology presented in this paper.

CHAPTER 2.
Mechanical Design

2.1 Spherical Mechanism Testbench

The spherical mechanism testbench is a device used to verify the performance of the mechanism and robot before applying it to humans and conducting clinical trials. The testbench consists of the off-board system, the exoskeleton robot model and the connecting components (Fig. 2.1). The power supply and controllers in the off-board system calculate the torque to be applied, and the motor transmits it to the robot model through the flexible drive shaft. The torque is relayed to the exoskeleton robot model, including the spherical mechanism, thigh imitating model, and the ball joint. The signals read by the sensors are transferred back to the controllers and saved in the storage device.

The exoskeleton robot model was designed to be applicable to various spherical mechanisms (Fig. 2.2). In this case, an aluminum-constructed R-4bar-R spherical mechanism which can generate 3-dimensional moment with only one directional rotation input [7] was used. The human's leg was imitated by a camera mounting ball joint (Horusbennu, FX-45T) for the hip joint, and a 3D printed thigh model covered by a 5mm silicon plate for compliance. Connection between the robot and human leg was made by thigh straps and 2.0 mm parachute cords, rigidly bonded without direct contact (Fig. 2.3 (b)) [8]. The ball joint was attached to an XYZ stage (DPIN, D3-412) to give factitious displacement of the hip joint, creating a misalignment with the spherical mechanism.

2.2 Actuator and Sensors

All parts of the actuator are located in the off-board system. AC servo motor (KOMOTEK, KAFZ-08DF6N21) was employed to drive the entire system, with the inclusion of a connected planetary gear (LS Electric, C3110103C16) featuring a gear ratio of 1:10. The Elmo's G-SOLTWIR50/100SE1H motor driver was utilized to transmit commands for motor operation and acquire motor feedback values.

The testbench has several sensors to calculate torques and detect angles. A torque sensor (FUTEK, TFF350, Fig. 2.4 (a)) is attached between the drive shaft and mechanism to determine the actual input moment. To measure the corresponding output moment, strain gauges (Fig. 2.4 (b)) are mounted to 20mm diameter aluminum tubes of both the imitated femur and exoskeleton robot, protected by 3D printed cases. Each pipe consists of 3-axis full Wheatstone bridge strain gauge, which detects combination moments associated with flexion/extension, abduction/adduction and internal/ external rotation. An IMU sensor (Xsens, MTi-

630, Fig. 2.4 (c)) is located inside a 3D printed mount which is attached with double-sided tape to a rigid part of the imitated human leg to measure current thigh angles. The torque sensor and strain gauges were calibrated by applying 2.0kg and 4.0kg weights to suitable directions for each situation to find the moment corresponding to the measured voltage value and to check the correlation coefficients between directions. The IMU sensor was initialized on a fixed location each time an experiment was proceeded.

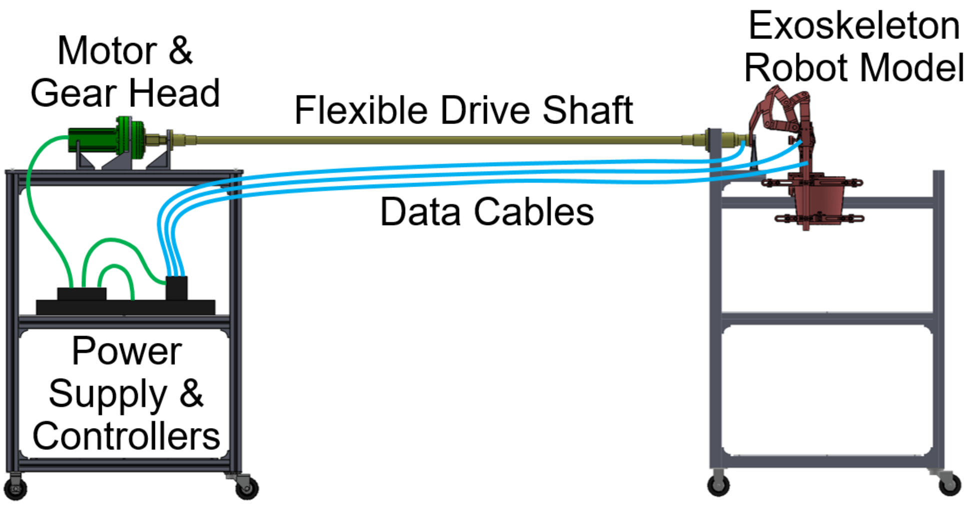

Fig. 2.1 The overall schematic diagram of the testbench shows that it consists of the offboard system and exoskeleton robot model, connected by flexible drive shaft and data cables in a configuration.

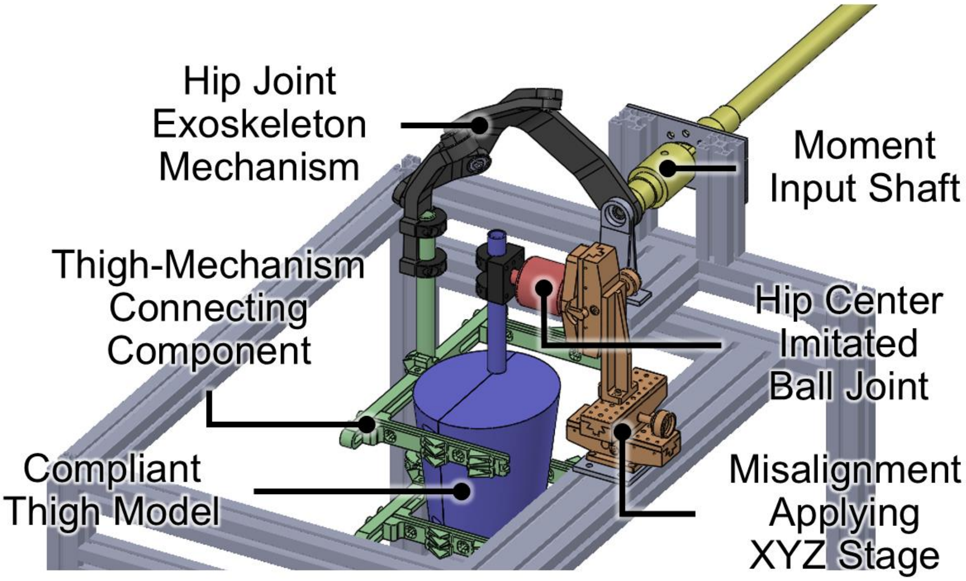

Fig. 2.2 The major components of the exoskeleton robot model in 3D design

` (a) (b)

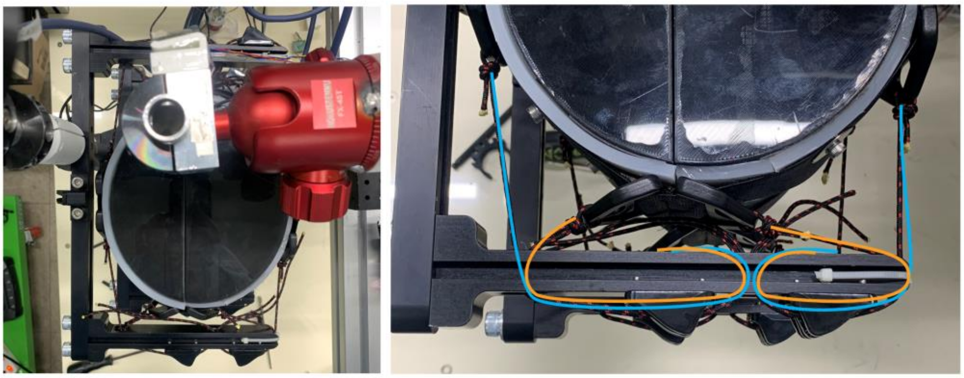

Fig. 2.3 (a) The configuration that connects the robot and the model's thigh. (b) One end of a parachute cable is connected to the buckle of thigh straps, and the other end is fixed to the clam cleat [8].

(a) (b) (c)

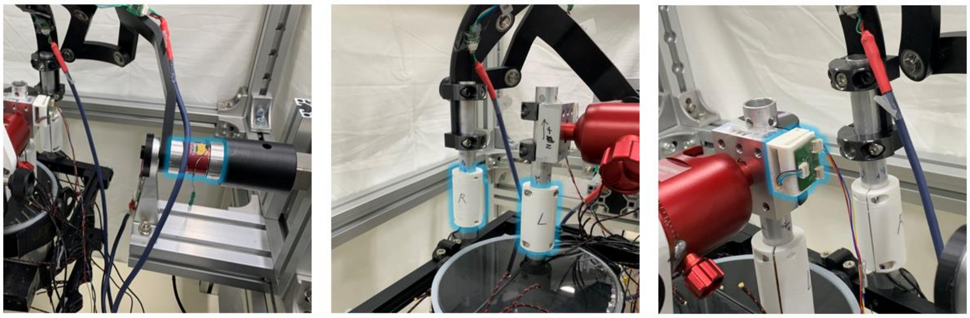

Fig. 2.4 Sensors that make up the testbench. (a) Torque sensor that reads the input moment. (b) Strain Gauge Wheatstone bridges that derives output moment, covered with 3D printed protection covers. (c) IMU sensor that pulls out real-time hip angles.

CHAPTER 3.
Experiment

3.1 Experiment Procedure

The experiment was conducted with the specification of a specific hip angle, intentional introduction of misalignment, and transmission of force using a motor. The hip angle was adjusted manually by shifting the thigh model while checking the IMU sensor value read in real-time. Once the desired position was reached, the ball joint was tightened to secure the hip angle in place. When applying misalignment, the fine adjustment screws on the XYZ stage were utilized to adjust in the order of Z, Y and X, with adjustments made in increments of 0.1mm. At the end of each experiment for each hip angle, misalignment was moved to the origin and then progressed.

The desired input moment was operated by the motor as a sequence in which a torque of -3.0 N·m was applied for 1 second at the start, gradually increased to +3.0 N·m for 5 seconds, maintained at +3.0 N·m for 1 second, and then released back to 0 N·m. The actual input moment obtained through the torque sensor was slightly skewed to the right compared to the desired moment (Fig. 3.1 (a)), due to the rise time delay. The strain gauge value was obtained by identifying the first occurrence of an actual moment exceeding 7 values as an index for each situation, which are moments ranging from -3.0 N·m to 3.0 N·m in 0.5 N·m intervals (Fig. 3.1 (b)).

3.2 Sampling Configuration

First, the experimental scope was defined for data collection required for modeling purposes. The method used in this process is Latin Hypercube Sampling (LHS). In the context of randomly selecting points within a workspace, the presence of a limited number of points can lead to a phenomenon of clustering towards one side. LHS resolves this issue by randomly selecting points while ensuring a uniform distribution, thus achieving a more even distribution of points. In order to define misalignment, ten points were selected within a uniform 11x11x11 workspace, covering a range of ± 20mm in the x, y, and z directions. (Fig. 3.2 (a), Table 3.1). For the hip angle, a workspace of size 15 × 10 was chosen to encompass the walking paths of 10 individuals, and similarly, 15 representative points were selected also using LHS (Fig. 3.2 (b),

Table **3.2**) [8].

(a)

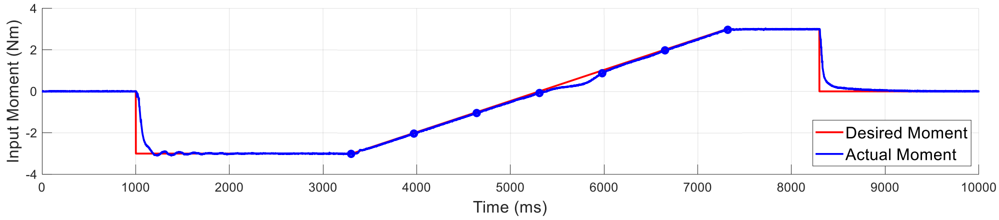

(b)

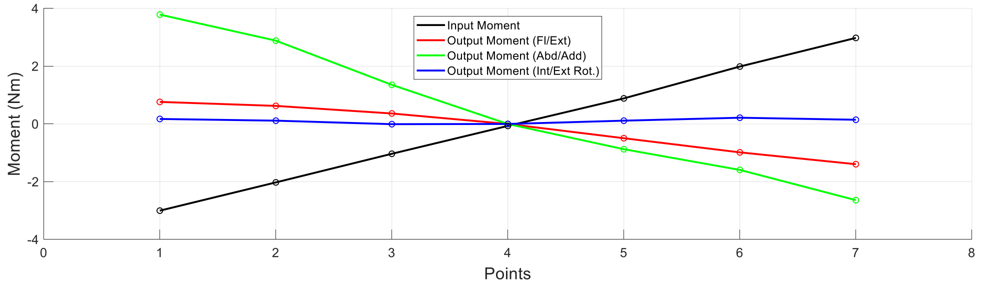

Fig. 3.1 (a) The desired(red) and actual(blue) input moments operated by the motor. 7 values with 0.5 N·m intervals were used to identify output moments. (b) Various moments in a single cycle of experiment include input moment read by the torque sensor(black), and output moments read by the strain gauge in the direction of flexion/extension, abduction/adduction, and internal/external rotation (red, green and blue in order)

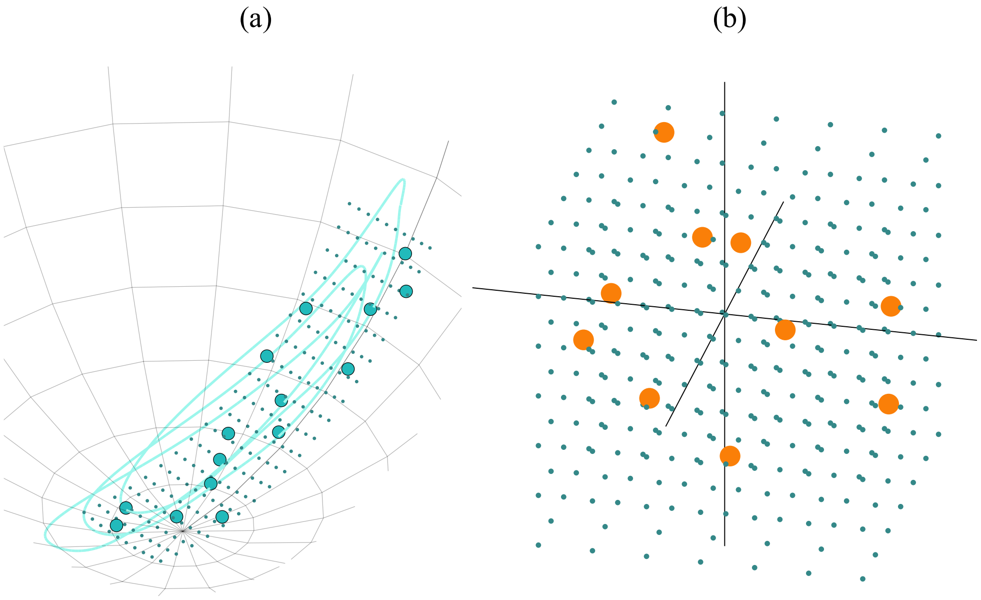

Fig. 3.2 Points chosen from workspace using Latin Hypercube Sampling(LHS) for (a) Hip angle points (b) Misalignment points

	Modeling (LHS)										Validation (Random)				
	1	**2**	**3**	**4**	**5**	**6**	**7**	**8**	**9**	**10**	**11**	**12**	**13**	**14**	**15**
X (mm)	10	-2	6	18	-10	2	-10	-6	14	-14	6	-18	0	16	4
Y (mm)	18	2	14	-14	6	-18	-6	-2	10	-10	-14	2	16	-12	-16
Z (mm)	-10	10	-2	-18	-6	2	18	-14	14	6	-2	2	12	-18	2

Table 3.1 Misalignment points for the experiments. 1-10 are modeling points created by Latin Hypercube Sampling (LHS). 11-15 are random points to validate the created model.

	1	2	3	4	5	6	7	8	9	10	11	12	13	14	15
Flexion	16.17	37.90	1.69	-5.55	27.04	34.28	23.41	45.14	30.66	19.79	8.93	-1.93	41.52	5.31	12.55
Adduction	-6.17	-4.41	-5.29	-0.87	0.02	-1.75	2.67	-7.94	1.79	-8.83	-7.06	-9.71	-2.64	0.90	-3.52
Rotation	0.18	0.18	0.18	0.18	0.18	0.18	0.18	0.18	0.18	0.18	0.18	0.18	0.18	0.18	0.18

Table 3.2 Hip angles for the experiments, created by Latin Hypercube Sampling from the workspace of 10 individual's gait trajectory [8].

	1	2	3	4	5	6	7	8	9	10
Flexion	32.60	27.84	17.31	6.96	-1.59	-7.19	-1.25	18.19	30.83	33.35
Adduction	-1.73	2.35	2.45	0.43	-0.30	-2.92	-8.88	-8.54	-4.32	-3.04
Rotation	-5.27	0.42	-1.11	-1.28	-3.30	-5.53	-0.62	3.66	9.57	-1.62

Table 3.3 Hip angle points for validation. These points represent the average of the gait data from 10 individuals, divided into 10 equal intervals. These were used for misalignment 11-13

CHAPTER 4.
Results

4.1 Testbench Reliability

In order to use the value derived from the sensor of the testbench for analysis, it must first be verified whether these values are reliable. The analytic hip moment was derived as follows:

$$\boldsymbol{r}_0 = \frac{(\boldsymbol{r}_2 \times \boldsymbol{r}_5) \times (\boldsymbol{r}_3 \times \boldsymbol{r}_4)}{\|(\boldsymbol{r}_2 \times \boldsymbol{r}_5) \times (\boldsymbol{r}_3 \times \boldsymbol{r}_4)\|} \tag{4.1}$$

$$\boldsymbol{M}_{out} = \frac{\boldsymbol{r}_0 \times \boldsymbol{r}_6}{\|\boldsymbol{r}_0 \times \boldsymbol{r}_6\|} \boldsymbol{M}_{inp} \tag{4.2}$$

where $\boldsymbol{r}_0 \sim \boldsymbol{r}_6$ are joints of the R-4bar-R mechanism (Fig. 1.1 (b)). Strain gauge moment was derived as follows:

$$\boldsymbol{M}_{SG} = \boldsymbol{X}(\alpha)\boldsymbol{Y}(\beta)\boldsymbol{Z}(\gamma)(V_{SG} - V_{SG}(\boldsymbol{M}_{T_{inp}=0})) \tag{4.3}$$

where α, β and γ are roll, pitch and yaw angles, and V_{SG} is the voltage from the strain gauge. The output moment obtained through the experiment ($\boldsymbol{M}_{SG}$) was compared with the theoretical values ($\boldsymbol{M}_{out}$) in the aligned state. As a result of analyzing the derived values, almost identical values were obtained (Fig. 4.1), which means that the experimental values using the testbench are reliable.

4.2 Correlation between Misalignment and Output Moment

By analyzing the difference between the values obtained with and without misalignment, it was observed that misalignment has an impact on the output. In a randomly selected misalignment condition, similar patterns of graphs were observed for all points along the gait trajectory, indicating consistent behavior (Fig. 4.2). Furthermore, when the experiment was conducted from a different misalignment, similar results were confirmed. Through this, it was observed that the output moment varies according to the changes in misalignment, and under the same misalignment conditions, similar output moment errors are obtained regardless of the hip angle.

4.3 Data Acquisition and Modeling

The data used in the model was divided into three types. The 3 hip angles from the IMU sensor and the input moment from the torque sensor was classified as ‘Input Data (X)’, whereas the 3 output moments read from the strain gauge called ‘Output data (Y)’. The misalignment in 3 directions which is used as a material as well as a prediction value was named ‘Hypothesis (θ)’. To build the desired model, Gaussian Process Regression (GPR) was utilized, input data (X) and hypothesis (θ) as an input and output data (Y) as an output (Fig. 4.3).

$$(\boldsymbol{X}, \boldsymbol{\theta}) \xrightarrow{model} \boldsymbol{Y} \tag{4.4}$$

$$\boldsymbol{X} \sim (IMU_{Roll}, IMU_{Pitch}, IMU_{Yaw}, TS)$$

$$\boldsymbol{Y} \sim (SG_{Fl}, \mathrm{SG}_{\mathrm{Ad}}, \mathrm{SG}_{\mathrm{Rot}})$$

$$\boldsymbol{\theta} \sim (Mis_x, Mis_y, Mis_z)$$

This method involves estimating the output value for a given input value through the examination of confidence intervals using diverse graphs that interpolate the experimentally acquired data points [8]. Given a constant specific misalignment, the IMU value and SG value exhibit dependency on the input torque. Consequently, the Gaussian Process Regression Model manifests as a single plane in space, while three separate planes arise based on the individual IMU values (Fig. 4.5).

4.4 Centroid Alignment Process

In order to validate the proposed model, it was necessary to once again determine the experimental scope. 5 random misalignment points were selected for validation and corresponding hip angles were also newly defined. For misalignments 11-13, 10 intervals of average gait data from 10 individuals were employed (Table 3.3), and for misalignments 14-15, hip angles used in model processing was once again used (Table 3.1).

The source of the GPR is the input data (X), meaning it is a real-time sensor data. The GPR model uses the three strain gauge models from **Fig. 4.3**, and maximum likelihood estimation (MLE). By these processes, a misalignment value is predicted, as shown in equation (Fig. 4.4)

$$\widehat{\boldsymbol{\theta}} = \underset{\boldsymbol{\theta}}{\operatorname{argmax}} \; [\, \boldsymbol{Y}^{*} - mdl(\boldsymbol{X}^{*}, \boldsymbol{\theta}) \,] \tag{4.5}$$

where $\widehat{\boldsymbol{\theta}}$ is misalignment prediction, and $\boldsymbol{X}^{*}, \boldsymbol{Y}^{*}$ are given values of X, Y. We validated the misalignment derived from the proposed model by comparing it with the actual values (Table 4.1). The sine value of the angle between prediction and actual misalignment was defined as similarity. The similarity varied from 65% to 99%, while the average was 86.73%. Since 3 out of 5 cases showed an accuracy of over 90%, it was judged that the accuracy of the model was at a level that could help correct misalignment.

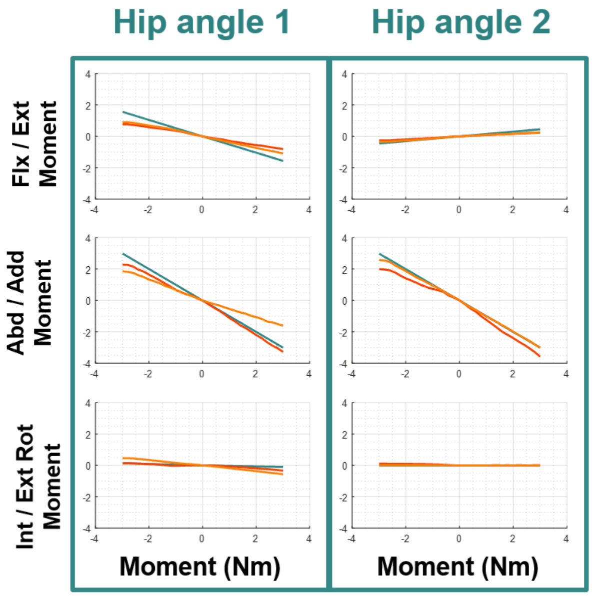

Fig. 4.1 Analytic hip moment (green), robot strain gauge moment (yellow), and hip strain gauge moment (orange) from three angles in 2 different hip angles.

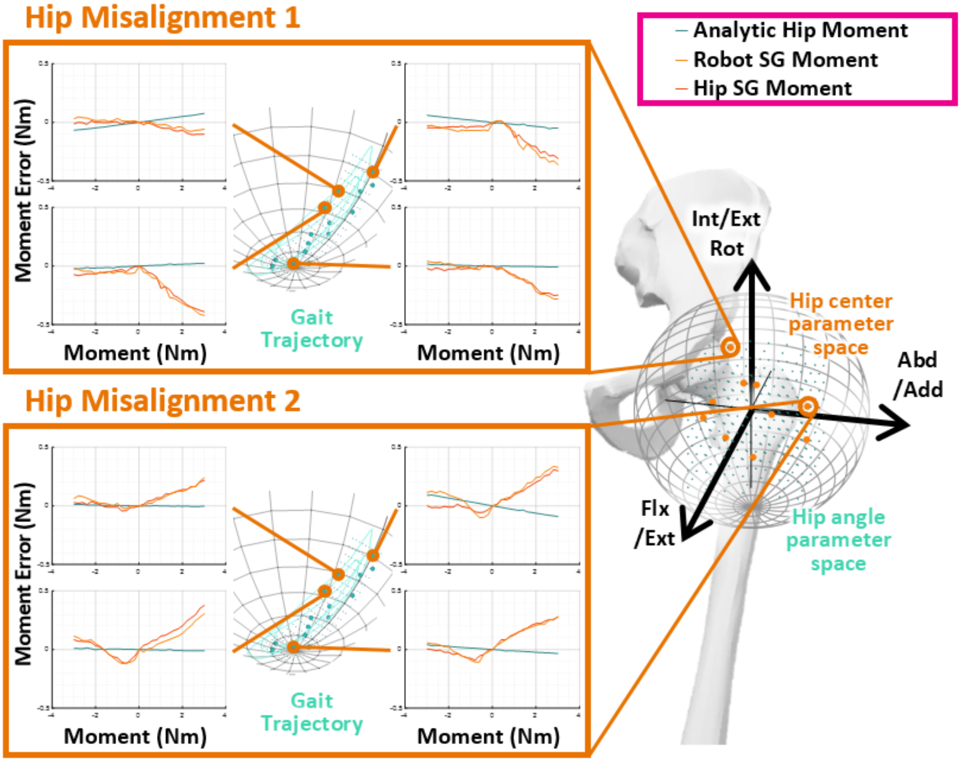

Fig. 4.2 Moment errors on points on the gait trajectory for two random misalignment points. In the same misalignment condition, similar patterns of graphs are observed for all points along the gait trajectory.

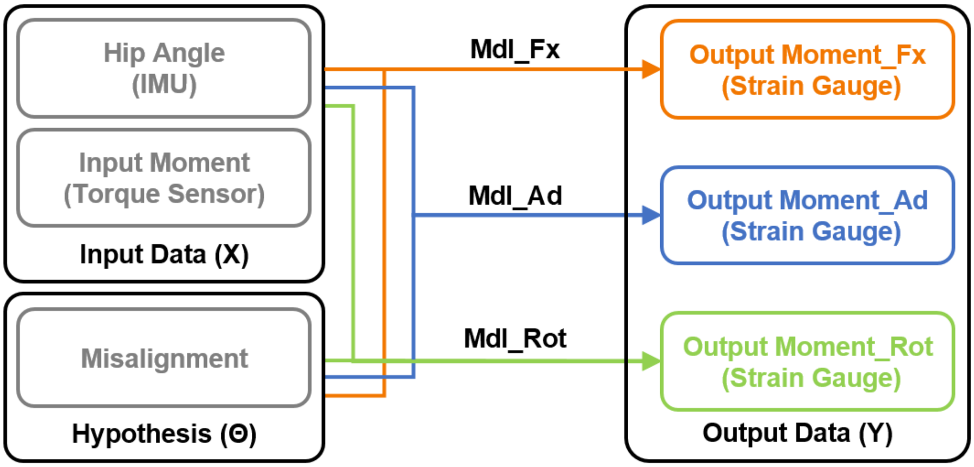

Fig. 4.3 The framework of Gaussian Process Regression (GPR) model. Input data (X) and hypothesis (θ) is inserted into the model which extracts output moments for 3 directions as the output data (Y)

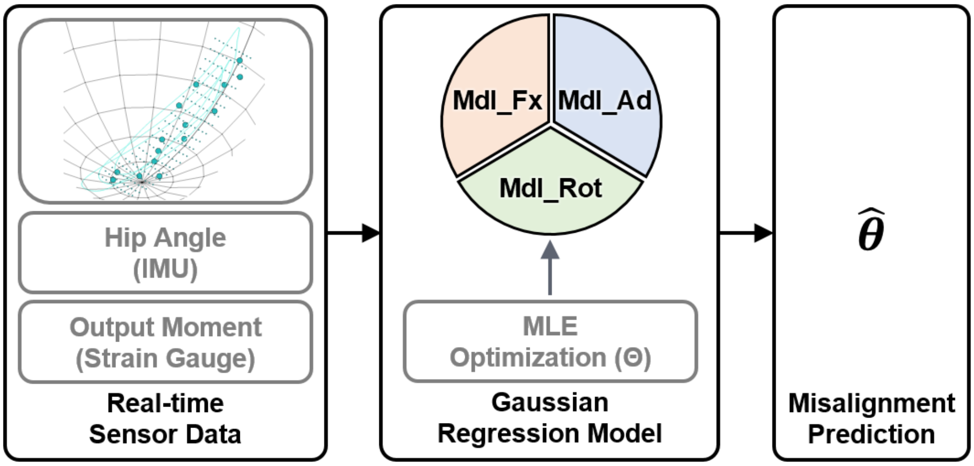

Fig. 4.4 The framework of the validation process. Real-time sensor data is inserted into Gaussian Process Regression (GPR) model, so that a prediction of misalignment can be derived.

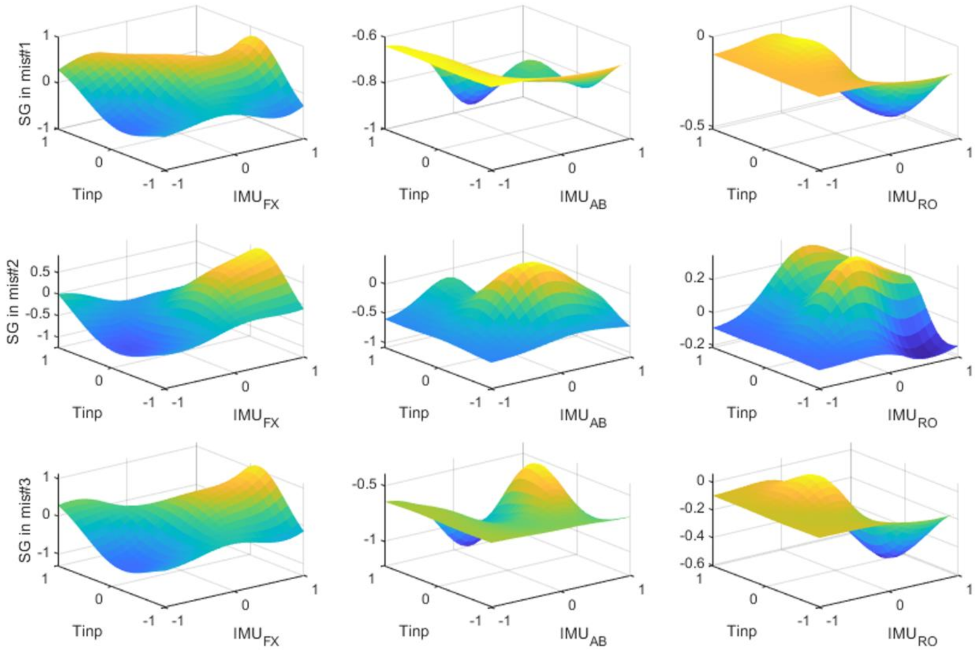

Fig. 4.5 Gaussian Process Regression model of all three strain gauges in one of the experimental situations.

		X	Y	Z	Similarity
11	Predict	0.3882	-0.8997	0.1873	**0.9494**
	Actual	0.3333	-0.7778	-0.1111	
12	Predict	-0.4033	0.0578	0.0893	**0.9939**
	Actual	-1.0000	0.1111	0.1111	
13	Predict	0.8564	0.8271	0.2609	**0.6598**
	Actual	0.0000	0.8889	0.6667	
14	Predict	0.5260	-0.7938	-0.4528	**0.9196**
	Actual	0.8889	-0.6667	-1.0000	
15	Predict	-0.5149	-0.7313	-0.3608	**0.8139**
	Actual	0.2222	-0.8889	0.1111	

Table 4.1 Comparison of predicted misalignment from proposed model and actual misalignment

CHAPTER 5.
Conclusion

This study presented a new methodology to improve efficiency by predicting and correcting the degree and direction of misalignment. Foremost, it was confirmed that the manufactured testbench and the configured experiment were a reliable environment. Upon analyzing the derived misalignment results, it can be concluded that the proposed model in this paper is valid. By using this model, misalignment can not only be determined in the testbench but also expected to be accurately assessed in a real robot applied to an actual person. This approach offers the advantage of real-time misalignment estimation, as it relies solely on the sensors embedded in the robot without the need for external markers or motion-capturing camera devices. Therefore, in future research, it is anticipated that studies will focus on correcting misalignment during walking and verifying its effectiveness. Moreover, it is believed that this model can be utilized in various ways, such as other hip joint exoskeleton mechanisms, diversity of protocols such as inclined walking or running, and robots with totally different joints, as long as there are sensors capable of reading the output moments in real-time.

REFERENCES

[1] J. K. Proud, D. T. Lai, K. L. Mudie, G. L. Carstairs, D. C. Billing, A. Garofolini, and R. K. Begg, “Exoskeleton application to military manual handling tasks,” Human Factors: The Journal of the Human Factors and Ergonomics Society, vol. 64, no. 3, pp. 527–554, 2020.

[2] J.-R. R. Diego, D. W. Martinez, G. S. Robles, and J. R. Dizon, “Development of smartphone-controlled hand and arm exoskeleton for persons with disability,” Open Engineering, vol. 11, no. 1, pp. 161–170, 2020.

[3] D. Zanotto, Y. Akiyama, P. Stegall, and S. K. Agrawal, “Knee joint misalignment in exoskeletons for the lower extremities: Effects on user's gait,” IEEE Transactions on Robotics, vol. 31, no. 4, pp. 978–987, 2015.

[4] M. B. Yandell, J. R. Tacca, and K. E. Zelik, “Design of a low profile, unpowered ankle exoskeleton that fits under clothes: Overcoming practical barriers to widespread societal adoption,” IEEE Transactions on Neural Systems and Rehabilitation Engineering, vol. 27, no. 4, pp. 712–723, 2019.

[5] M. E. Harrington, A. B. Zavatsky, S. E. M. Lawson, Z. Yuan, and T. N. Theologis, “Prediction of the hip joint centre in adults, children, and patients

with cerebral palsy based on Magnetic Resonance Imaging," Journal of Biomechanics, vol. 40, no. 3, pp. 595–602, 2007.

[6] M. T. Goldsmith, M. T. Rasmussen, T. L. Turnbull, C. A. C. Trindade, R. F. LaPrade, M. J. Philippon, and C. A. Wijdicks, "Validation of a six degree-of-freedom robotic system for hip in vitro biomechanical testing," Journal of Biomechanics, vol. 48, no. 15, pp. 4093–4100, 2015.

[7] S. W., Kang, "Novel topology optimization formulation for wearable motion/force transmitting robot mechanisms having general joints," Ph.D. dissertation, Dept. Mech. Eng., Seoul Nat'l Univ., Seoul, Republic of Korea, 2020.

[8] V. L. Chiu, M. Raitor, and S. H. Collins, "Design of a hip exoskeleton with actuation in frontal and sagittal planes," IEEE Transactions on Medical Robotics and Bionics, vol. 3, no. 3, pp. 773–782, 2021. doi:10.1109/tmrb.2021.3088521

[9] E. Schulz, M. Speekenbrink, and A. Krause, A tutorial on gaussian process regression: *Modelling, exploring, and exploiting functions,* 2016. doi:10.1101/095190

ABSTRACT (KOREAN)

고관절 외골격 로봇의 중심 정렬을 위한 구면 메커니즘의 성능 평가 및 조정

이 규 익
서울대학교 대학원
기계항공공학부

인체 관절과 로봇 관절의 회전 중심 사이의 오정렬은 효율성과 안전성에 상당한 영향을 미칠 수 있다. 하지만 고관절은 자유도가 높고 회전 중심이 몸 안쪽에 위치하기에 이러한 오정렬이 발생할 확률이 상대적으로 높다. 본 연구에서는 내부 센서만을 이용하여 고관절의 정확한 위치를 예측하는 새로운 방법론을 제안하였다. 오정렬을 인위적으로 부여할 수 있는 테스트벤치를 제작하고, R-4bar-R (R4R) 구조의 구형 메커니즘을 사용하여 이 방법을 검증하였다. 출력 모멘트와 오정렬의 상관관계를 이용하여 맵핑 시스템을 구축하여 오정렬을 역추적할 수 있도록 하였으며, 이를 위해 가우시안 프로세스 회귀를 활용하여 모델을 구축하였다.

주요어: 외골격로봇, 고관절, 오정렬 예측, 보정 방법론, 스트레인 게이지 휘트스톤 브리지, 구형 메커니즘, 라틴 하이퍼큐브 샘플링, 가우시안 프로세스 회귀

학 번 : 2021-20088